

Accepted Manuscript

Lanthanide(Tb^{3+} , Eu^{3+})-functionalized a newonedimensional Zn-MOF composite as luminescent probe for highlyselectively sensing Fe^{3+}

Yi Wang, Rui Huang, Jiaojiao Zhang, Gang Cheng, Huan Yang

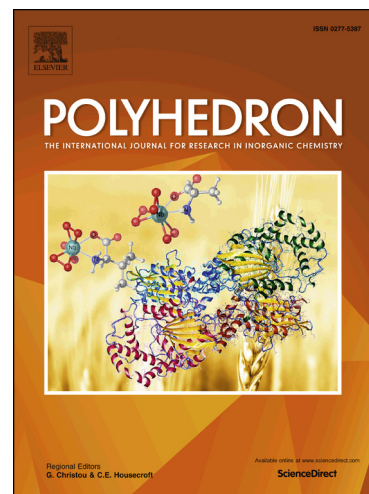
PII: S0277-5387(18)30181-5
DOI: <https://doi.org/10.1016/j.poly.2018.04.013>
Reference: POLY 13115

To appear in: *Polyhedron*

Received Date: 13 February 2018
Accepted Date: 9 April 2018

Please cite this article as: Y. Wang, R. Huang, J. Zhang, G. Cheng, H. Yang, Lanthanide(Tb^{3+} , Eu^{3+})-functionalized a newonedimensional Zn-MOF composite as luminescent probe for highlyselectively sensing Fe^{3+} , *Polyhedron* (2018), doi: <https://doi.org/10.1016/j.poly.2018.04.013>

This is a PDF file of an unedited manuscript that has been accepted for publication. As a service to our customers we are providing this early version of the manuscript. The manuscript will undergo copyediting, typesetting, and review of the resulting proof before it is published in its final form. Please note that during the production process errors may be discovered which could affect the content, and all legal disclaimers that apply to the journal pertain.



Lanthanide(Tb^{3+} , Eu^{3+})-functionalized a new one-dimensional Zn-MOF composite as luminescent probe for highly selectively sensing Fe^{3+}

Yi Wang¹, Rui Huang², Jiaojiao Zhang¹, Gang Cheng¹, Huan Yang^{2*}

¹College of chemistry and Material Engineering, Gui Yang University, 550005, Guiyang, P.R. China

²School of Material science and Engineering Han Shan Normal University, Chaozhou, 521041, P.R. China

E-mail: yanghuanjx@163.com

A new one dimensional zinc metal organic framework $\{[Zn(NDIC)\cdot 2H_2O] \cdot 2H_2O\}_n$ ((NDIC = 5-(5-Norbornene-2,3-dicarboximide)Isophthalic acid) has been synthesized under an hydrothermal condition and chosen as a parent framework to sensitize via encapsulating Tb^{3+} and Eu^{3+} cations in Zn-MOF. The obtained composite $Tb(3+)\@Zn-MOF$ shows excellent luminescence which performs a remarkable quenching effect in the luminescence emission of Tb^{3+} upon the introduction of Fe^{3+} . Subsequently, $Tb(3+)\@Zn-MOF$ as a highly selective and sensitive sensor for Fe^{3+} . Most importantly, the luminescence probe of Fe^{3+} shows a low detection limit ($7.5\times 10^{-6}M$), a broad linear range ($2.5\times 10^{-6}-7.5\times 10^{-5}$). A paper strip coated with $Tb(3+)\@Zn-MOF$ material was also shown to be highly selective for Fe^{3+} and under the irradiation of UV light of 254 nm by the naked eyes. This is first example for detecting metal ions based on a lanthanide functionalized a new Zn metal-organic framework.

1. Introduction

Metal-organic frameworks (MOFs) have emerged a crystalline hybrid materials obtained constructed by the assembly of metal ions/clusters and organic linkers, and have been emerging as very promising multifunctional materials, such as catalysis,[1-3] magnetism,[4,5] gas storage and separation,[6-8] energy storage.[9-11] As a subfamily of MOFs reported, Ln-MOFs have been receiving great attention due to their lots of fascinating luminescence properties such as high quantum yield, relatively long life time, characteristic sharp-line emissions and large Stokes shifts.[12-14] The combination of these excellent optical properties together with diverse structures and topologies of MOFs offers an effective platform for chemical sensing. In the past decade, there are many researches on luminescent Ln-MOFs for sensing, such as metal ions,[15-17] anions,[18,19] small molecules[20-23] and temperature[24-26] have been reported. It is a great challenge to design and synthesis of the targeted Ln-MOFs via direct synthesis due to the higher coordination number and various coordination modes of lanthanide ions. Postsynthetic modification method of MOFs provides an way to exploit and expand their unique properties. The conventional incorporation of photoactive Ln^{3+} into the channels of MOFs hosts may produce new luminescent signals at different positions. It will offer a new possibility to realize the multiband emissions originated from different Ln^{3+} and perform the similar luminescent sensing function of lanthanide MOFs.[27,28]

Fe^{3+} ion is the most abundant transition element for either humans or other living organisms on account of their significance in basic and essential biological processes and systems.[29,30] Either deficient or excessive Fe^{3+} from the normal permissible limit can lead to serious system disorder. The damages to cells may further leading to many kinds of disorders, such as cancer, Parkinson's diseases and Alzheimer's disease. Moreover, Fe^{3+} is also a common inorganic pollutant. Excessive Fe^{3+} could result in lots of diseases related to human health. [31] Therefore, the selective detection of Fe^{3+} is a very necessary in biological research and the development of selective detection or sensing of iron over other metal ions seems to be very important for human health. In fact, many works have been successfully reported the sensing of Fe^{3+} . However, there are only a few luminescent sensors selective

for Fe^{3+} , simultaneously, without the interference of other mixed metal ions via luminescence quenching is still a challenge now.[32]

In this work, a new metal organic framework $\{[\text{Zn}(\text{NDIC})\cdot 2\text{H}_2\text{O}] \cdot 2\text{H}_2\text{O}\}_n$ was designed and obtained via solvothermal reactions. Subsequently, A novel luminescence hybrid composite of lanthanide-doped Zn-MOF($\text{Tb}(3+)\text{@Zn-MOF}$) was constructed through encapsulating Tb^{3+} cations in Zn-MOF. What is more, $\text{Tb}(3+)\text{@Zn-MOF}$ is used as highly selective and sensitive luminescent sensor for Fe^{3+} among many other metal ions in ethanol solution. The possible sensing mechanisms were discussed in detail. As expected, $\text{Tb}(3+)\text{@Zn-MOF}$ is suitable for becoming one luminescent probe for Fe^{3+} with high selectivity and sensitivity.

2. Materials and methods

All the reagents and solvents were purchased from different companies, and directly used as received without further purification.

Single crystal X-ray crystallography

A colorless single crystal of Zn-MOF was sealed in a capillary tube with the some mother liquor inside in order to prevent desolvation of the crystal Data for the crystal was collected using graphite monochromated Mo K α radiation ($\lambda=0.71073$ Å) at 293 K on Rigaku Oxford CCD diffractometer. The absorption corrections were applied by using the multiscan program, the structure were solved by direct methods and refined with on F^2 by least-squares technique with the program SHELXTL-2016. The refinement of structural model were performed with anisotropic displacement parameters restraints, such as DFIX, SIMU, AFIX, ISOR for the benzene rings and solvent molecules. Graphics were generated using Diamond 3.0. The crystallographic data and details of refinements and the selected bond lengths and angles for Zn-MOF are listed in Table 1, 2 and S2.

IR absorption spectra of the Zn-MOF and $\text{Tb}(3+)\text{@Zn-MOF}$ were performed on a IR Affinity-1 FT-IR spectrometer by dry KBr slices in the wavenumber range of 400–4000 cm^{-1} . The amounts of metal ions in $\text{Tb}(3+)\text{@Zn-MOF}$ (Tb:Zn) and $\text{Eu}(3+)\text{@Zn-MOF}$ (Eu:Zn) were determined by inductively coupled plasma mass spectrometry (ICP-MS, Icap Qc, Thermo-Fisher, Germany) Powder X-ray diffraction (PXRD) patterns were performed coupled with Cu K α radiation (1.5418 Å) on a Rigaku Miniflex 600 X-ray diffractometer at room temperature. Thermogravimetric analysis (TGA) was measured under nitrogen protection from 50 °C to 700 °C with a heating rate of 5 °C min^{-1} on a Netzsch sta 449f3. Luminescence spectra were recorded on Horiba ihr320 fluorescence spectrophotometer at room temperature. The emission quantum yield was recorded on FLS980 Fluorescence Spectrofluorometer at room temperature, the luminescent lifetime of $\text{Tb}(3+)\text{@Zn-MOF}$ was recorded on FLS920 Fluorescence Spectrofluorometer.

Synthesis of $\{[\text{Zn}(\text{NDIC})\cdot 2\text{H}_2\text{O}] \cdot 2\text{H}_2\text{O}\}_n$ (Zn-MOF)

$\text{Zn}(\text{CH}_3\text{COO})_2$ (0.1 mmol, 18.3 mg) and NDIC (0.05 mmol, 0.0165 g) were dissolved in 3 mL DMF. The mixture was sealed in 15 mL solvothermal vessel, and was subsequently heated at 80 °C for 3 days then a gradual cooling procedure to room temperature. The resulting colorless prism crystals were obtained in 65% yield based on NDIC.

Preparation of lanthanide (Tb^{3+} , Eu^{3+})@Zn-MOF

Powder of Zn-MOF (100 mg) is soaked in ethanol solution of $\text{Tb}(\text{NO}_3)_3\cdot 6\text{H}_2\text{O}$ and $\text{Eu}(\text{NO}_3)_3\cdot 6\text{H}_2\text{O}$ (10 mL, 2 mmol) for 1 day respectively. The resulting white solid was then separated from the mixed dispersion by centrifugation and washing with ethanol to remove redundant Tb^{3+} and Eu^{3+} , the resulted white powder was dried at 60 °C for 6 h. The ratio of Tb:Zn and Eu:Zn is 1:16 and 1:20, respectively.

Luminescence Sensing Experiment

2 mg powder of Tb(3+@Zn-MOF were dispersed into ethanol solution (4 mL, 1×10^{-3} molL⁻¹) of M(NO₃)_x (Mⁿ⁺ = Ag⁺, Pb²⁺, Mg²⁺, Cd²⁺, K⁺, Zn²⁺, Ni²⁺, Co²⁺, Fe³⁺) at room temperature, and then the mixture was equilibrated thoroughly for 5 min by ultrasound processing. The mixtures were used for luminescence measurements. All the luminescence data were recorded at the room temperature.

3. Results and discussion

3.1 Description of crystal structure

Zn-NDIC (1) crystallizes in the space group P21/c, and the asymmetric unit comprises one Zn²⁺ ion, one bridging NDIC²⁻, two coordinated water molecules, and two guest water molecule. As shown in Figure 1, the Zn²⁺ ion is five-coordinated by three carboxylate oxygen atoms from two NDIC²⁻ [Zn-O1=1.907(9)Å, Zn-O4a=2.048(1)Å, Zn-O3a=2.417(2)Å] and two oxygen atoms of two coordinated water molecules [Zn-O7=2.007(6)Å, Zn-O8=1.957(8)Å] to generate a distorted square pyramid coordination geometry. The Zn centers are bridged by NDIC to forming one chain dimensional structure (Figure 1b), chains are bridged by hydrogen bond (Table 2) forming three dimensional structure (Figure 1c).

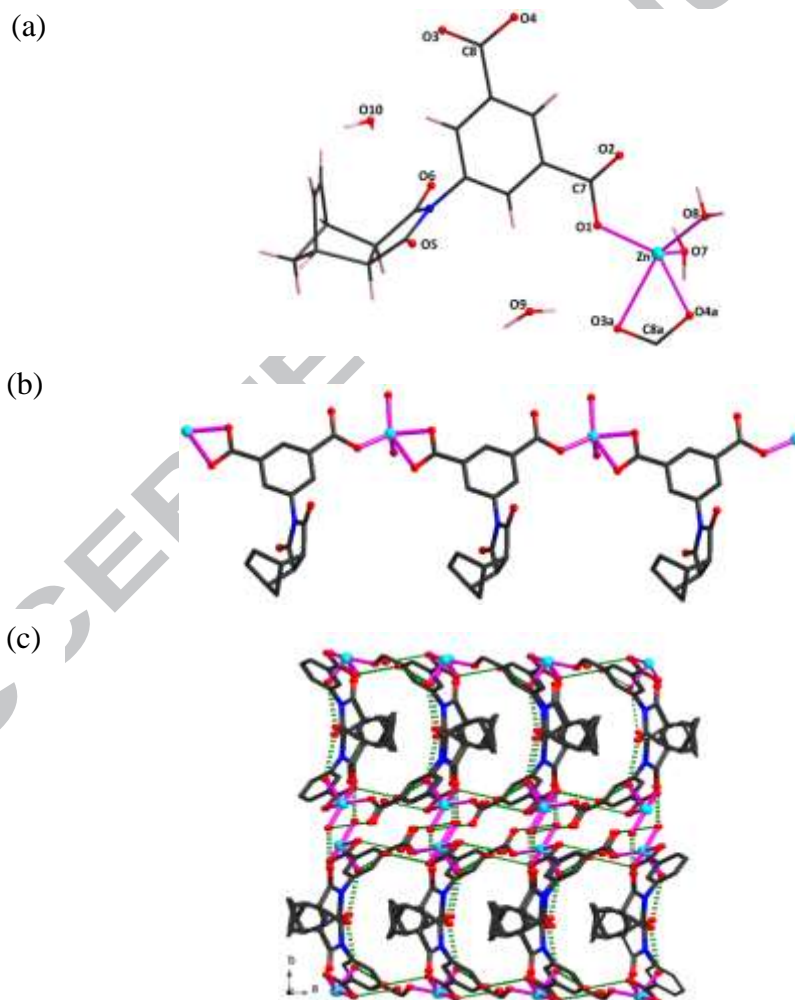


Figure 1 (a) Asymmetric unit of Zn-MOF (b) One-dimensional structure of Zn-MOF

(c) Three-dimensional structure of Zn-MOF

Table 1. Crystal data and structure refinement for Zn-MOF.

Compound	Zn-MOF
Chemical Formula	C ₁₇ H ₁₇ NO ₁₀ Zn
Formula weight	462.75
Crystal system	Monoclinic
Space group	P2(1)/c
<i>a</i> (Å)	7.8480(8)
<i>b</i> (Å)	23.377(3)
<i>c</i> (Å)	12.2665(13)
α (°)	90
β (°)	126.687(7)
γ (°)	90
<i>V</i> (Å ³)	1804.7(4)
<i>Z</i>	4
<i>D_c</i> (g/cm ³)	1.703
μ (mm ⁻¹)	1.347
<i>T</i> (K)	293(2)
Wavelength (Å)	1.54178
<i>F</i> (000)	950
Crystal size (mm)	0.21 × 0.08 × 0.07
Absorption coefficient	2.445 mm ⁻¹
Data / restraints	2677 / 6
Parameters	262
<i>F</i> (000)	950
<i>R</i> ₁ indices [<i>I</i> > 2σ(<i>I</i>)]	0.0799
<i>wR</i> ₂ indices [<i>I</i> > 2σ(<i>I</i>)]	0.1015
<i>R</i> ₁ indices [all data]	0.2472
<i>wR</i> ₂ indices [all data]	0.1682

Table 2 Hydrogen-bond geometry (Å)

	d(D···A)	∠(DHA)
O10-H10B···O4#3	2.889(9)	166.9
O9-H9B···O3#1	2.820(8)	160.9
O9-H9A···O7#3	2.654(7)	167.4
O8-H8B···O5#2	2.884(8)	123.9
O8-H8A···O2	2.992(7)	126.8

Symmetry transformations used to generate equivalent atoms: #1 *x*+1,*y*,*z*+1; #2 -*x*+2,-*y*+2,-*z*+1; #3 *x*-1,*y*,*z*.

3.2 Purity and thermal stability

In order to explore application of Zn-MOF, the purity and thermal stability of the material were investigated. Figure 2(a) shows the PXRD patterns of the Zn-MOF and Tb(3+)-@Zn-MOF from 5° to 50°, the PXRD pattern of as prepared Zn-MOF (CCDC: 1819140) is well matched with the simulated data, which indicates a high purity of the Zn-MOF. The PXRD pattern of the Tb(3+)-@Zn-MOF and Eu(3+)-@Zn-MOF are also in agreement with the simulated Zn-MOF (Figure S2). The result shows that

the preparation of Tb(3+@Zn-MOF and Eu(3+@Zn-MOF are successful and the crystallinity of Zn-MOF could retain still kept original crystal type. The Zn-MOF and Tb(3+@Zn-MOF was monitored by TG analysis. The TG curve of the Zn-MOF in Fig. 2b presents two events. The first weight loss below 140°C is ascribed to the release of the surface water molecules. The range from 140 °C to 400 °C corresponds to the loss of ligand. Afterwards, The final plateau from 540 °C corresponds to zinc oxide. The Tb@Zn-MOF was also monitored by TG analysis from 0 to 700 °C (Figure 2b). The TGA of Tb@Zn-MOF exhibits two events of weight losses and shows good thermal stability similar to Zn-MOF. The first step occurs below 140 ° C is ascribed to the release of the surface water molecules. The second weight loss from 150 ° C to 400 ° C corresponds to the decomposition of the organic ligand. The final plateau from 540 ° C corresponds to oxide.

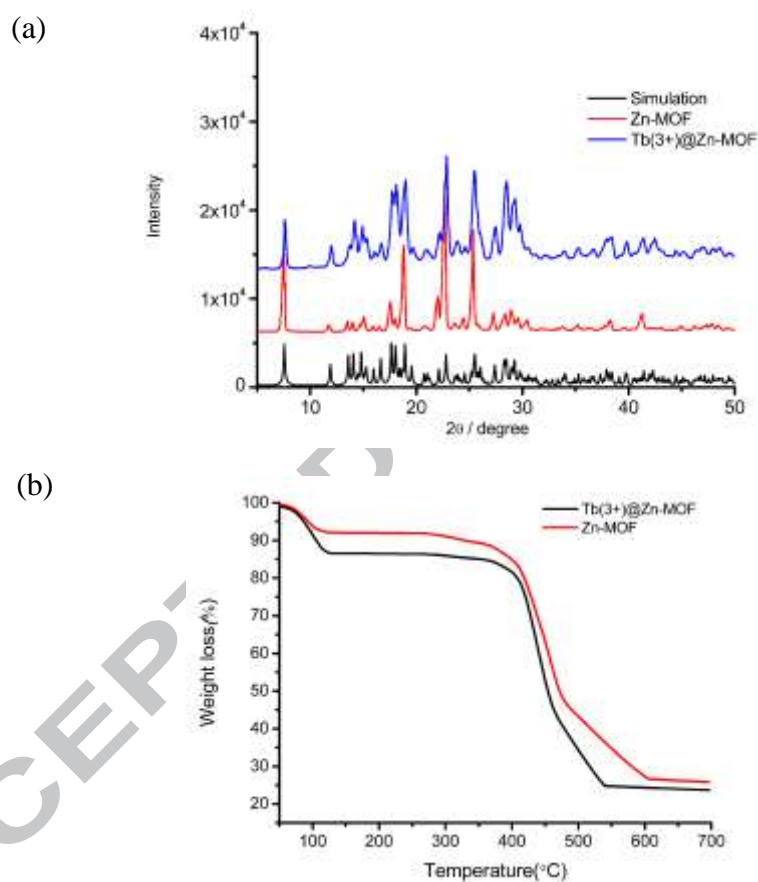


Fig. 2 (a) Powder X-ray diffraction patterns of simulated Zn-MOF, prepared Zn-MOF and Tb(3+@Zn-MOF. (b) TGA of prepared Zn-MOF and Tb(3+@Zn-MOF.

As shown in Figure 3, the peaks that are located 1680 cm^{-1} and 1359 cm^{-1} are ascribed to the absorption of $\nu_{\text{C=O}}$ in Zn-MOF. Subsequently, Zn-MOF was immersed in ethanol solution of $\text{Tb}(\text{NO}_3)_3$ for Tb^{3+} -encapsulation in the channels by connecting to the uncoordinated-COOH of Zn-MOF. the absorption band of Zn-MOF show a significant red-shift (about 10 nm) after connecting to Tb^{3+} , indicating the interactions between the Tb^{3+} and free-COOH of Zn-MOF. After incorporation of Tb^{3+} into the Zn-MOF, the hybrid composite not affect the crystalline integrity of Zn-MOF, as shown by the PXRD patterns (Figure 2a).

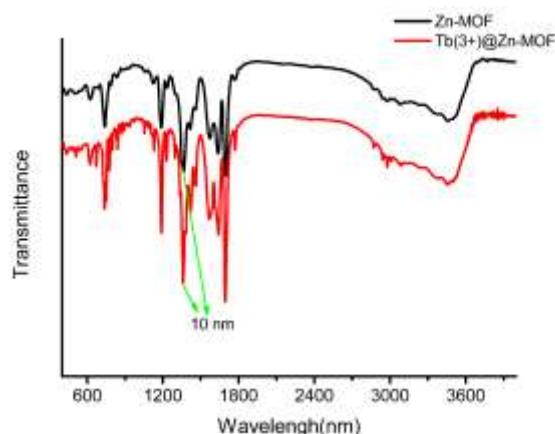


Fig. 3 IR spectra of Zn-MOF and Tb(3+)@Zn-MOF

3.3 Luminescence Properties of Tb(3+)@Zn-MOF

In Fig.4, when excited at 303 nm, the emission spectrum of the Tb(3+)@Zn-MOF exhibits characteristic emission of Tb³⁺. The sharp lines located at about 489, 545, 592 and 612 nm can be ascribed to ⁵D₄ → ⁷F_J (J = 3–6) transitions of Tb³⁺. Eu(3+)@Zn-MOF also exhibit the characteristic emission bands of Eu³⁺ ions at 580, 594, 618 nm (⁵D₀ → ⁷F_J)(J = 0–2) in the PL spectra(Fig. S3). [33, 34] Under UV-light irradiation, Tb(3+)@Zn-MOF and Eu(3+)@Zn-MOF shows strong green and red luminescence which can be observed by naked eye, the results shows that the antenna effect occurs. The emission quantum yield and average lifetime of Tb(3+)@Zn-MOF is 42.67% and 0.587 ms.

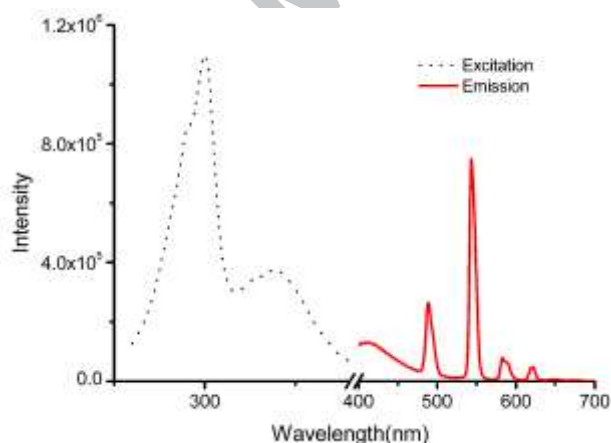


Fig. 4 The excitation (dashed) and emission (solid) spectra of the Tb(3+)@Zn-MOF.

3.4 Detection of cations

To explore the potential of Tb(3+)@Zn-MOF for detection of metal ions, the responses of the luminescence emission of Tb(3+)@Zn-MOF to different cations were investigated. The powder of Tb(3+)@Zn-MOF was dispersed in an ethanol solution of 0.001 mol L⁻¹ M(NO₃)_x (M = Ag⁺, Pb²⁺, Mg²⁺, Cd²⁺, K⁺, Zn²⁺, Ni²⁺, Co²⁺, Fe³⁺ respectively) and ultrasonicated over 5 min to form the metal ion incorporated (MOF-Mⁿ⁺) suspension. The luminescent intensities were recorded at room temperature in Figure 5(a). Interestingly, the results are that the luminescent intensities of them are greatly dependent on the metal ions. For example, as shown in Figure 5(b), the luminescence intensity at 545 nm is decreased when Zn²⁺, Na⁺, K⁺, Mg²⁺, Ni²⁺, Ag⁺, Co²⁺ are introduced. In the contrast, the luminescence intensity increased when Ag⁺, Pb²⁺, Cd²⁺ are introduced. Meanwhile, the Fe³⁺ shows a significant quenching effect on the luminescence intensity of Tb(3+)@Zn-MOF. The above results indicate that the Tb(3+)@Zn-MOF is promising chemical sensor for Fe³⁺.

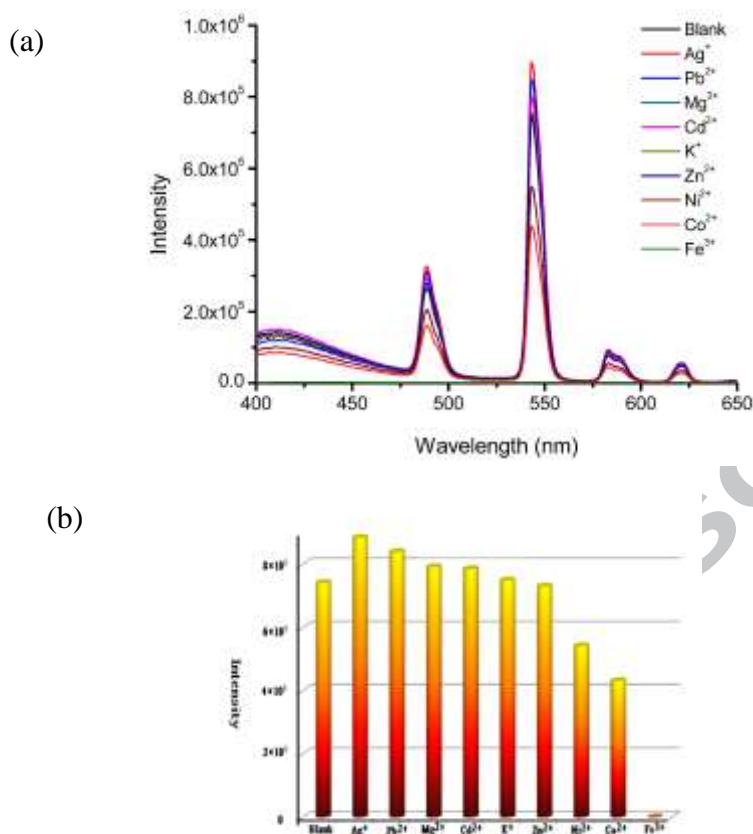


Fig. 5 (a) Emission spectra and (b) The luminescence intensities at 545 nm of the Tb(3+)@Zn-MOF in various metal ions

To better prove that the luminescence quenching by Fe^{3+} , concentration-dependent studies in the luminescence intensities of Tb(3+)@Zn-MOF when concentration of Fe^{3+} ions increased were carried out. As shown in Figure 6a and 6b, the luminescence intensity of the Tb(3+)@Zn-MOF decreases with the increase of Fe^{3+} concentration from 2.5×10^{-6} – 7.5×10^{-5} M. The linear correlation coefficient (R^2) in the K_{sv} curve of Tb@Zn-MOF with Fe^{3+} is 0.99679, this quenching effect can be rationalized by the Stern-Volmer equation:[35;36]

$$I_0/I = 1 + K_{sv}[M]$$

Where the values I and I_0 represent the luminescence intensities of the Tb(3+)@Zn-MOF with and without the presence of Fe^{3+} , respectively, $[M]$ represents the Fe^{3+} concentration. K_{sv} is the quenching constant, the value is calculated as $1.57 \times 10^4 \text{M}^{-1}$, which reveals a strong quenching effect on the Tb(3+)@Zn-MOF luminescence. The detection limit is about $7.5 \times 10^{-6} \text{M}$ ($\Delta S/N=3$). [37] The results suggest that Fe^{3+} also can be detected quantitatively using Tb@Zn-MOF.

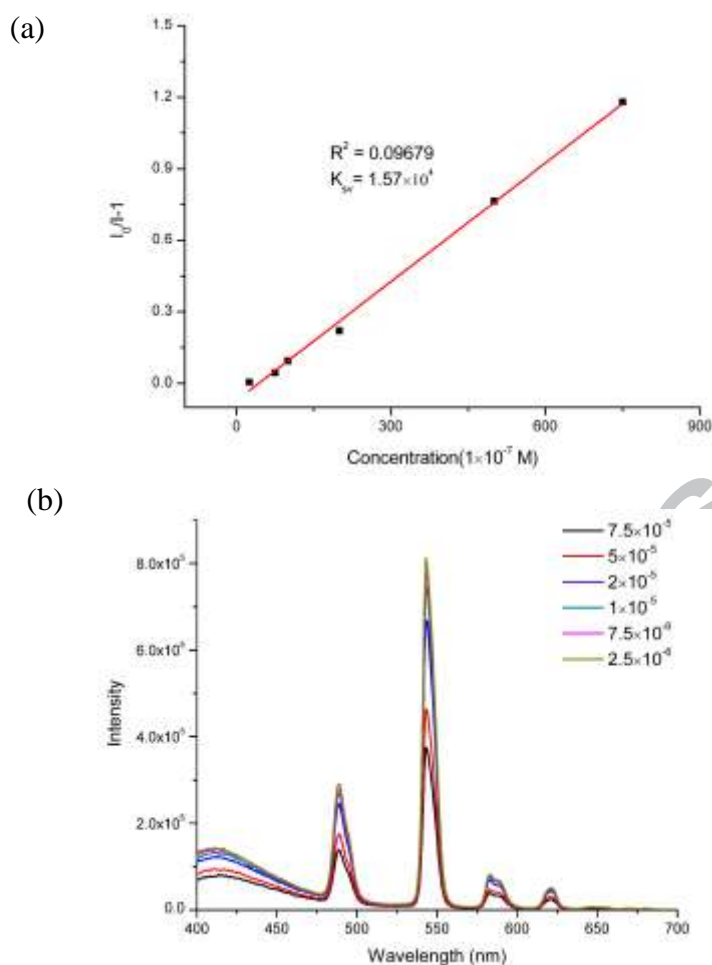


Fig. 6 (a) Stern–Volmer plots describe the dependency of the luminescent intensities on the Fe^{3+} concentration over the range of 2.5×10^{-6} – 7.5×10^{-5} M in ethanol solution. (b) Luminescence emission spectra of $\text{Tb}(3+)\text{@Zn-MOF}$ dispersed in ethanol upon incremental addition of Fe^{3+} (2.5×10^{-6} – 7.5×10^{-5} M) ethanol solution ($\lambda_{\text{ex}} = 303$ nm).

As shown in Fig. 7, the $\text{Tb}(3+)\text{@Zn-MOF}$ is dispersed in the solution containing Fe^{3+} and other metal ions, which include Ag^+ , Pb^{2+} , Mg^{2+} , Cd^{2+} , K^+ , Zn^{2+} , Ni^{2+} , Co^{2+} , respectively. When excited at 303 nm, the $\text{Tb}(3+)\text{@Zn-MOF}$ is immersed in the mixed ions (1×10^{-3} M other metal ions + 1×10^{-3} M Fe^{3+}), the measurement of the luminescence intensity shows that the luminescence is completely quenched, indicating that the selectivity for Fe^{3+} is not interfered by the existence of other ions.

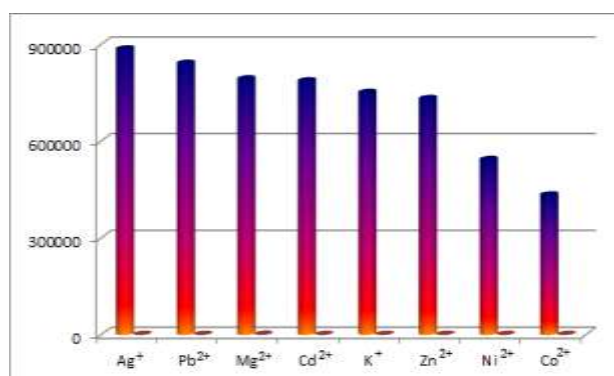


Fig. 7 Luminescence intensities at 545 nm of the Tb(3+@Zn-MOF upon the addition of different metal ions(1×10^{-3} M) (colors) and subsequent addition of Fe³⁺(1×10^{-3} M) (red) (λ_{ex} = 303 nm).

3.5 Engineering filter paper based sensor devices

The simple, rapid and naked eye detecting ability of the probe provided us the opportunity to develop a user-friendly and low-cost detection device for the analysis of Fe³⁺. A luminescence test paper was fabricated for rapid detection of cations. We prepared test paper by immersing a filter paper (2.0×1.0 cm²) in the ethanol solution of Tb(3+@Zn-MOF (1×10^{-3} M) and drying it in air at room temperature. For the detection of Fe³⁺, the paper was immersed in the ethanol solution of cations (1×10^{-3} M, Ag⁺, Pb²⁺, Mg²⁺, Cd²⁺, K⁺, Zn²⁺, Ni²⁺, Co²⁺, Fe³⁺) and then dried in air. In Figure 8, under the irradiation of UV light of 254 nm, the luminescent colors of the test paper changed from green to dark green, and finally black with the different metal ions. Considering the results above, we can distinguish the colors of different metal ions by our naked eyes.



Fig. 8 Luminescent response of Tb(3+@Zn-MOF coated paper strips to various cations(1×10^{-3} M) under UV light (254nm) (left to right: Ag⁺, Pb²⁺, Mg²⁺, Cd²⁺, K⁺, Zn²⁺, Ni²⁺, Co²⁺, Fe³⁺).

3.6 Quenching mechanism

Up to date, the mechanisms for such quenching effects of cations is attributed to four reasons: (1) the interaction between targeted metal ions and MOFs; (2) the exchange between lanthanide ions and central metal ions of MOFs (3) the collapse of the crystal structure.(4) the energy competition between linker and cations.[35, 38,39]Herein, to elucidate the possible sensing mechanism for the quenching effect of Fe³⁺ on the luminescence of Tb(3+@Zn-MOF, the PXRD was employed to study on the structural data of the Tb(3+@Zn-MOF with and without treated with Fe³⁺. As shown in Figure 9, the PXRD of Tb(3+@Zn-MOF with and without treated with Fe³⁺ is different, suggesting that the basic frameworks of Tb(3+@Zn-MOF changed. We speculate that the quenching effect of Tb(3+@Zn-MOF by Fe³⁺ is attributed to the collapse of the framework.

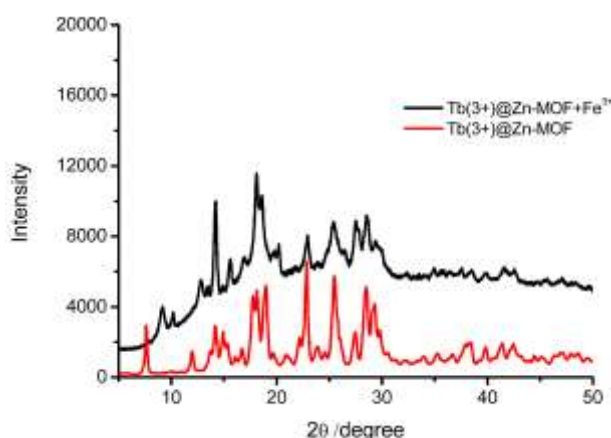


Fig.9 PXRD patterns of simulated Zn-MOF and Tb(3+@Zn-MOF treated with iron ions.

4. Conclusions

In summary, a new one dimensional Zn-MOF{[Zn(NDIC)·2H₂O] ·2H₂O}_n has been prepared and chosen as host to sensitize Tb³⁺ and Eu³⁺ by uncoordinated-COOH group in its channels. This composite has excellent luminescence property and thermostability. Studying of the luminescence properties reveals that Tb(3+)-@Zn-MOF can develop as a highly selective and sensitive sensor for Fe³⁺(detection limit, 7.5×10⁻⁶M) via luminescence quenching of Tb³⁺. Practically, luminescence test paper was fabricated and treated with different cations, the colors have changed from green to dark under the irradiation of UV light, respectively. The present results may provide a facile route to design luminescence Ln-MOF based on new Zn MOF for sensing and further studies are currently under way.

Appendix A. Supplementary data

CCDC <1819140> contains the supplementary crystallographic data for Zn-MOF. These data can be obtained free of charge via <http://www.ccdc.cam.ac.uk/conts/retrieving.html>, or from the Cambridge Crystallographic Data Centre, 12 Union Road, Cambridge CB2 1EZ, UK; fax: (+44) 1223-336-033; or e-mail: deposit@ccdc.cam.ac.uk.

Acknowledgements

The authors acknowledge the financial support of project of Guizhou youth science and technology talents (20170695104), Chaozhou science and technology plan (2016GY22), Experimental Teaching Demonstrating Center of Guizhou province (science and education Experimental Teaching Demonstrating Center of Guiyang university).

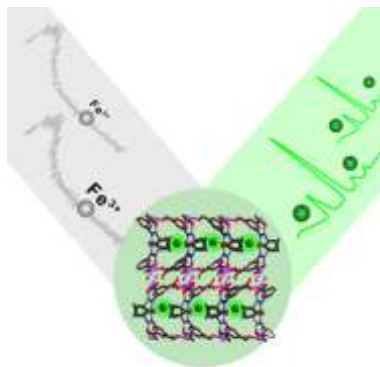
References

1. J. W. Liu, L. F. Chen, H. Cui, J. Y. Zhang, L. Zhang, C.Y. Su. *Chem. Soc. Rev.*, 43(2014) 6011-6061.
2. C. D. Wu, A. G. Hu, L. Zhang, W. B. Lin. *J. Am. Chem. Soc.*, 127(2005) 8940-8941.
3. Y. Liu, W. Xuan, Y. Cui. *Adv. Mater.*, 22(2010) 4112-4135.
4. G. E. Mínguez, E. Coronado. *Chem. Soc. Rev.*, 47(2018) 533-557.
5. Y. M. Shao, L. C. Zhou, Chao Bao, Junjun Ma, M. Z. Liu, F. Wang. *Chem. Eng. J.*, 283(2016) 1127-1136.
6. D. N. Dybtsev, H. Chun, S. H. Yoon, D. W. Kim, K. Kim. *J. Am. Chem. Soc.* 126(2004) 32-33.
7. M. Dinca, A. F. Yu, J. R. Long. *J. Am. Chem. Soc.*, 128(2006) 8904-13.
8. B. Xiao, P. S. Wheatley, X. B. Zhao, A. J. Fletcher, S. Fox, A. G. Rossi, I. L. Megson, S. Bordiga, L. Regli, K. M. Thomas, R. E. Morris. *J. Am. Chem. Soc.*, 129(2007), 129:1203-1209.
9. Y. Zhao, Z. X. Song, X. Li, Q. Su, N. C. Cheng, S. Lawes, X. L. Sun. *Energy Storage Materials*, 2(2016) 35-62.
10. L. Wang, X. Feng, L. T. Ren, Q. H. Piao, J. Q. Zhong, Y. B. Wang, H. W. Li, Y. F. Chen, B. Wang. *J. Am. Chem. Soc.*, 137(2015) 4920-4923.
11. S. N. Guo, Y. Zhu, Y. Y. Yan, Y. L. Min, J. C. Fan, Q. J. Xu, H. Yun, *J. Power Sources*, 316(2016) 176-182.
12. L. V. Meyer, F. Schoenfeld, K. MuellerBuschbaum. *Chem. Comm.*, 2014, 50(60):8093-8108.
13. B. Li, H. M. Wen, Y. J. Cui, G. D. Qian, B. L. Chen. *Adv. Mater.*, 2016, 28(40)8819-8860.
14. D. E. Barry, D. F. Caffrey, T. Gunnlaugsson. *Chem. Soc. Rev.*, 45(2016) 3244-3274.
15. P. Y. Du, W. Gu, X. Liu. *Inorg. Chem.*, 55(2016) 7826-7828.
16. B. Ding, S. X. Liu, Y. Cheng, C. Guo, X. X. Wu, J. H. Guo, Y. Y. Liu, Y. Li. *Inorg. Chem.*, 55(2016) 4391-4402.
17. Q. S. Wang, J. J. Li, M. N. Zhang, X. Li, *Sensors Actuat B: Chem.*, 258(2018) 358-364
18. Q. B. Bo, H. T. Zhang, H. Y. Wang, J. L. Miao, Z. W. Zhang. *Chem. Eur. J.*,

- 20(2014) 3712-3723.
19. K. L. Wong, G. L. Law, Y. Y. Yang, W. T. Wong, *Adv. Mater.* 18(2006) 1051–1054.
20. J.M. Zhou, H.H. Li, H. Zhang, H.M. Li, W. Shi, P. Cheng, *Adv. Mater.* 27(2015), 7072-7077.
21. Z. S. Qin, W. W. Dong, J. Zhao, Y. P. Wu, Q. C. Zhang, D. S. Li. *Inorg. Chem. Frontiers*,5(2017)120-126.
18. Z. Hu, B. J. Deibert, J. Li. *Chem. Soc. Rev.*, 2014, 43(16):5815
19. S. Dang, X. Min, W.T. Yang, F. Y. Yi, H. P. You, Z. M. Sun. *Chem. Eur. J.*, 19(2013) 17172-17179.
20. Y. J. Cui, H. Xu, Y. F. Yue, Z. Y. Guo, J. C. Yu, Z. X. Chen, J. K. Gao, Y. Yang, G. D. Qian, B. L. Chen. *J. Am. Chem. Soc.*, 134(2012) 3979-82.
21. Y. J. Cui, F. L. Zhu, B. L. Chen, G. D. Qian. *Chem. Commun.*, 2015, 51, 7420-7431.
22. Y. J. Cui, R. J. Song, J. C. Yu, M. Liu, Z. Q. Wang, C. D. Wu, Y. Yang, Z. Y. Wang, B. L. Chen, G. D. Qian. *Adv. Mater.* 27(2015) 1420-1425.
23. Y. Wang, F. Zhang, Z. S. Fang, M. H. Yu, Y. Y. Yang, K. L. Wong, *J. Mater. Chem. C*, 4(2016) 8466 - 8472.
24. Z. S. Dou, J. C. Yu, Y. J. Cui, Y. Yang, Z. Y. Wang, D. R. Yang, G. D. Qian. *J. Am. Chem. Soc.*, 136(2014) 5527–5530.
25. S. Biswas, V. Sharma, P. Kumar, A. L. Koner, *Sensors Actuat B: Chem.*, 260(2018) 460-464.
26. A. Kanaan, T. D. Nguyen, H. Dallaporta, J. M. Raimundo, A. M. Charrier. *Anal. Chem.*, 88(2016) 3804–3809.
27. R Dalapati, Ü KökçamDemir, C Janiak, S. Biswas. *Dalton Trans.*, 47(2018) 1159-1170.
28. M. Zheng, H. Q. Tan, Z. G. Xie, L. G. Zhang, X. B. Jing, Z. C. Sun. *ACS Appl. Mater. Interfaces*, 5(2013), 1078–1083.
29. Y. T. Yan, W. Y. Zhang, F. Zhang, F. Cao, R. F. Yang, Y. Y. Wang, L. Hou. *Dalton Trans.*, 47(2018) 1682-1692.
30. Y. Wang, H. Yang, G. Cheng, Y. Y. Wu, S. M. Lin. *CrystEngComm*, 19(2017) 7270-7276.
31. W. Liu, J. Xie, L. M. Zhang, M. A. Silver, S. A. Wang. *Dalton Trans.*, 47(2018) 649-653.
32. Y. Zhou, H. H. Chen, B. Yan, *J. Mater. Chem. A* 2(2014), 13691-13697.
33. H. Li, R. Lan, C. F. Chan, G. Bao, C. Xie, P.-H. Chu, W. C. S. Tai, J. X. Zhang and K. L. Wong, *Chem. Comm.*, 53(2017), 7084-7087.
34. G. L. Law, K. L. Wong, K. K. Lau, S. T. Lap, P. A. Tanner, F. C. Kuo, W. T. Wong, *J. Mater. Chem.* 20(2010) 4074-4079.
35. X. Y. Xu, B. Yan. *ACS Appl. Mater. Interfaces*. 7(2015) 721-729.
36. H. N. Abdelhamid, A. B. Gmez, B. Martín-Matute, X. D. Zou. *Microchimica Acta*, 184(2017), 3363-3371.
37. Y. M. Zhu, C. H. Zeng, T. S. Chu, H. M. Wang, Y. Y. Yang, Y. X. Tong, C. Y. Su, W. T. Wong, *J. Mater. Chem. A*, 1(2013) 11312-11319.
38. C. X. Yang, H. B. Ren, X. P. Yan. *Anal. Chem.* 85(2013) 7441-7446.
39. S. T. Zhang, J. Yang, H. Wu, Y. Y. Liu, J. F. Ma. *Chem. Eur. J.* 21(2015) 15806-15819.

TOC

Lanthanide(Tb^{3+} , Eu^{3+})-functionalized a new one dimensional Zn-MOF. The composite $Tb(3+)@Zn-MOF$ performs luminescence emission of Tb^{3+} and shows a remarkable quenching effect upon the introduction of Fe^{3+} .



A new Zinc metal organic framework has been synthesized and chosen as a parent framework to sensitize via encapsulating Tb^{3+} cations in Zn-MOF. The obtained composite $Tb(3+)@Zn-MOF$ shows excellent luminescence which performs a remarkable quenching effect in the luminescence emission of Tb^{3+} upon the introduction of Fe^{3+} .